Title: A biosensor based on gold nanoparticles, dihexadecylphosphate, and tyrosinase for the determination of catechol in natural water

Author: Fernando Campanhã Vicentini Lívia L.C. Garcia Luiz C.S. Figueiredo-Filho Bruno C. Janegitz Orlando Fatibello-Filho

PII: S0141-0229(15)30087-9
DOI: http://dx.doi.org/doi:10.1016/j.enzmictec.2015.12.004
Reference: EMT 8842

To appear in: *Enzyme and Microbial Technology*

Received date: 7-5-2015
Revised date: 3-12-2015
Accepted date: 9-12-2015

Please cite this article as: Campanhã Vicentini Fernando, Garcia Lívia LC, Figueiredo-Filho Luiz CS, Janegitz Bruno C, Fatibello-Filho Orlando.A biosensor based on gold nanoparticles, dihexadecylphosphate, and tyrosinase for the determination of catechol in natural water.*Enzyme and Microbial Technology* http://dx.doi.org/10.1016/j.enzmictec.2015.12.004

A biosensor based on gold nanoparticles, dihexadecylphosphate, and tyrosinase for the determination of catechol in natural waters

Fernando Campanhã Vicentini[a,b,*], Lívia L. C. Garcia[a], Luiz C. S. Figueiredo-Filho[a,c], Bruno C. Janegitz[a], Orlando Fatibello-Filho[a]

[a]*Department of Chemistry, Federal University of São Carlos, Rod. Washington Luís km 235, P. O. Box 676, 13560-970 São Carlos - SP, Brazil*

[b]*Center of Nature Sciences, Federal University of São Carlos, Rod. Lauri Simões de Barros km 12, 18290-000 Buri - SP, Brazil*

[c]*Federal Institute of Paraná, Câmpus Paranavaí - Rua José Felipe Tequinha 1400 - Jardim das Nações, 87703-536 Paranavaí - PR, Brazil*

* Corresponding author: Department of Chemistry, Federal University of São Carlos, P. O. Box 676, São Carlos 13560-970, SP, Brazil, Tel +55 16 33518070; Fax +55 16 33518350

Email: fercv02@yahoo.com.br

Highlights

- A new biosensor is proposed using a GCE modified with Au nanoparticles and Tyr within DHP
- The proposed electrode can be easily prepared and showed low detection limit
- The Tyr-AuNPs-DHP/GCE was successfully applied for catechol determination in fresh water samples

Abstract

In this work, a biosensor using a glassy carbon electrode modified with gold nanoparticles (AuNPs) and tyrosinase (Tyr) within a dihexadecylphosphate film is proposed. Cystamine and glutaraldehyde crosslinking agents were used as a support for Tyr immobilization. The proposed biosensor was characterized by scanning electron microscopy (SEM), transmission electron microscopy (TEM), and cyclic voltammetry in the presence of catechol. The determination of catechol was carried out by amperometry and presented a linear concentration range from 2.5×10^{-6} to 9.5×10^{-5} mol L^{-1} with a detection limit of 1.7×10^{-7} mol L^{-1}. The developed biosensor showed good reproducibility and stability. Moreover, this novel amperometric method was successfully applied in the determination of catechol in natural water samples. The results were in agreement with a 95% confidence level for those obtained using the official spectrophotometric method.

Keywords: *Tyrosinase biosensor, Gold nanoparticles, Dihexadecylphosphate, Catechol determination, Amperometry.*

1. Introduction

Metallic nanoparticles have been extensively used in recent years in several technologic devices [1-3]. In electroanalysis, nanoparticles have been applied for electrode modification, due to advantages, such as their electrocatalytic effect and improved active area and mass transport [2, 4]. These advantages can provide a better analytical performance in comparison with bulk electrodes [5-8]. Furthermore, for the development of new biosensors, gold nanoparticles (AuNPs) show good mechanical resistance and electrical properties, and have large active surface areas for enzyme immobilization (which increases the number of attached biocomponents in the sensing surface), and good biocompatibility [5, 9]. Thus, several studies have explored the use of AuNPs in combination with biomolecules for the development of new architectures for biosensors [10-12].

Some phenolic compounds are toxic pollutants that present a potential hazard for human health and aquatic life [13, 14]. They often enter the aquatic environments via industrial residues from different kinds of production, such as plastics, dyes, drugs, resins, pesticides, and especially paper and cellulose [15, 16]. The use of new biosensors for the detection of phenolic compounds has advantages, such as rapid response, shorter analysis times since there is no need sophisticated sample treatment, low cost, simplicity of preparation, and high sensitivity and selectivity. Different kinds of architecture for biosensors to detect phenolic compounds can be found in the literature, including dual-enzyme systems, immunosensors, nucleic acid biosensors, and enzyme-based biosensors (tyrosinase, laccase, and horseradish peroxidase)[17].

Tyrosinase (Tyr) is also known as polyphenol oxidase or catechol oxidase, and has two copper atoms in its active center [15]. This important enzyme catalyzes oxidation reactions, including the hydroxylation of monophenols to *o*-dihydroxy

phenols, and subsequently, the oxidation-dihydroxy phenols to o-quinones in the presence of molecular oxygen [18].

A critical step in the development of biosensors is how to immobilize the enzyme efficiently without any modification to the active center or denaturation. In recent years, a wide range of surface-linking methods have been developed, including physical adsorption [19], occlusion via gel encapsulation [20, 21], electrochemical entrapment of enzymes within a polymer or a composite matrix [22-24], covalent bonds [11, 12, 25], and covalent crosslinking [24, 25].

Dihexadecylphosphate (DHP) is a surfactant that presents a negatively charged phosphatic polar head and two long hydrophobic tails, and does not form micelles [26]. This material can be dispersed in water by ultrasonic agitation, and its dispersion can form a very stable film on electrode surfaces, which is similar to stacks of biomembranes. The film formation probably occurs via hydrogen bonds, and has been used in the development of sensors [27-29] and biosensors [30-33].

In this paper, we report a new biosensor using Tyr enzyme immobilized covalently in a film containing AuNPs and DHP on a glassy carbon electrode (GCE) to determine catechol concentrations by amperometry in natural water samples.

2. Experimental

2.1. Chemicals and reagents

Hydrogen tetrachloroaurate (III), 25% v/v glutaraldehyde, cystamine, dihexadecylphosphate (DHP), sodium citrate, and tyrosinase 50 kU (from mushroom), 4-aminoantipyrine, and catechol (99%) were purchased from Sigma–Aldrich. All other chemicals were of analytical grade and were used as received. A 0.01 mol L^{-1} catechol stock solution (prepared daily) was made in a 0.1 mol L^{-1} phosphate buffer solution (pH

6.0), which was obtained using Na_2HPO_4 and NaH_2PO_4. All solutions were prepared using nanopure water (resistivity > 18.2 MΩ cm) from a Millipore Milli-Q system (Billerica, USA). The 0.1 mol L^{-1} phosphate buffer solution was employed as the supporting electrolyte in all the measurements with the biosensor.

2.2. Apparatus

The electrochemical measurements were recorded with a three-electrode system, including the biosensor Tyr-AuNPs-DHP/GCE as the working electrode, a platinum plate as the counter electrode, and Ag/AgCl (3.0 mol L^{-1} KCl) as the reference electrode at 25ºC, to which all potentials are hereinafter referred. Electrochemical measurements were carried out using an Autolab Ecochemie model PGSTAT12 (Utrecht, Netherlands) potentiostat/galvanostat controlled by GPES 4.9 software.

The morphology and the size of AuNPs were characterized by scanning electron microscopy (SEM) using a Zeiss DSM 940A and transmission electron microscopy (TEM) using a FEG Zeiss Supra 35-VP equipment with electron beam energy of 20 keV. Histograms were constructed using the public-domain ImageJ image-processing software.

For comparison, the catechol determination was also performed spectrophotometrically [34] using a Femto spectrophotometer (model 435, Brazil) with a quartz cuvette (optical path length of 10 mm) set at 500 nm.

2.3. Synthesis of AuNPs

The AuNPs colloidal solution was prepared by citrate reduction of $HAuCl_4$ in aqueous solution by the Turkevich method [35]. Initially, we added 4.0 mL of 0.05 mol L^{-1} $HAuCl_4$ in 200 mL of water at 90°C under stirring. Then, 2.0 mL of 0.3 mol L^{-1}

sodium citrate solution was added, and the mixture was stirred for 4 min at 90°C until the appearance of a red color. Finally, the reaction was rapidly cooled to room temperature in an ice bath.

2.4. Gold nanoparticles dispersion

AuNPs dispersion was prepared by dispersing 1.0 mg of DHP in 1.0 mL of AuNPs colloidal solution. The dispersion was subjected to ultrasonication for 30 min. In addition, for comparison, we constructed one film containing 1.0 mg of DHP in 1.0 mL of nanopure water in the same way.

2.5. Preparation of the Tyr-AuNPs-DHP/GCE biosensor

The GCE (diameter 5 mm) was polished sequentially with metallographic abrasive paper (No. 6) and slurries of 0.3 μm alumina microparticles to a mirror finish. After being rinsed with nanopure water, the electrode was sonicated in isopropyl alcohol for 3 min and then with nanopure water for a further 3 min, and then dried at room temperature. Afterwards, 20 μL of AuNPs-DHP dispersion was casted onto the GCE, and the solvent was allowed to evaporate at room temperature for 2 h. The electrode was named AuNPs-DHP/GCE. After that, the AuNPs-DHP/GCE was placed in the electrochemical cell containing 0.1 mol L^{-1} KCl, and 20 cycles in the potential range from −0.3 to 0.7 V at a scan rate of 100 mV s^{-1} were applied using cyclic voltammetry (CV). The electrode was carefully washed with nanopure water. Then, the AuNPs-DHP/GCE was modified with cystamine (CYS) and glutaraldehyde (GA) to link the Tyr covalently. Next, 20 μL of 10 mmol L^{-1} CYS solution was casted onto the electrode surface, and the solvent was evaporated at room temperature for 1 h, and was then was rinsed with 0.1 mol L^{-1} phosphate buffer solution (pH 6.0). Subsequently, 20

µL of 2.5% (v/v) GA solution was cast onto the surface of the AuNPs-DHP/GCE, and the solvent was evaporated at room temperature for 1 h. The electrode was washed with 0.1 mol L^{-1} phosphate buffer solution (pH 6.0). Finally, 20 µL of a solution containing 2000 units of Tyr in phosphate buffer solution (0.1 mol L^{-1}, pH 6.0) was cast onto the surface of the AuNPs-DHP/GCE, and the solvent was evaporated at room temperature for 2 hours. Thereafter, the electrode was thoroughly washed with phosphate buffer solution. The schematic process of the fabrication of the biosensor is presented in Fig. 1. When it was not in use, the Tyr-AuNPs-DHP/GCE was stored in phosphate buffer solution (0.1 mol L^{-1}, pH 6.0) in a refrigerator at 4ºC.

2.6. Samples and reference method

The samples from natural water (A−C) were collected from the lake at the Federal University of São Carlos, São Carlos city, Brazil. The collection points were recorded using a GPS (*A* = 21°59’08.06’’S 47°52’55.13’’W, *B* = 21°59’10.96’’S 47°52’52.16’’W, and *C* = 21°59’11.54’’S 47°52’42.63’’W). Each sample was prepared using an aliquot of 50 mL of the sample, which was transferred to different calibration flasks. Then, aliquots of catechol standard solution were carefully added to the samples and they were stirred in order to homogenize the solutions. The 4-aminoantipyrine spectrophotometric method [34] was performed to compare the results with those obtained by the Tyr-AuNPs-DHP/GCE method employing amperometry.

3. Results and Discussion

3.1. Characterization of AuNPs-DHP/GCE

Firstly, we characterized the stability of AuNPs-DHP. The addition of DHP to the AuNPs solution led to the production of a stable solution (data not shown), and this solution became an adherent film when it was casted onto the GCE. We employed SEM to characterize the AuNPs-DHP/GCE and GCE. Fig. 2 shows the GCE (a) and AuNPs-DHP/GCE (b) images, in which it can be observed that the AuNPs-DHP film was homogeneously distributed across the surface of the GCE. Furthermore, we used TEM to evaluate the AuNPs size. As can be seen in Fig. 2(c), the AuNPs presented an average diameter of 17.4 nm, as shown in the histogram (Fig. 2(d)).

We also characterized the AuNPs-DHP/GCE by cyclic voltammetry in 0.5 mol L^{-1} H_2SO_4 solution at 50 mV s^{-1}. We can observe in Fig. 3(a) that the modified electrode presented a classic redox voltammetric profile of gold with an anodic peak at 1.30 V and a cathodic peak at 0.84 V. Both peaks are related to gold oxide species formed on the electrode surface in the sulfuric acid that was the supporting electrolyte [36].

We also estimated the electroactive areas of the GCE and AuNPs-DHP/GCE in 0.1 mol L^{-1} KCl solution in the presence of 1.0 mmol L^{-1} $[Fe(CN)_6]^{4-}$ (diffusion coefficient of 6.2×10^{-6} cm^2 s^{-1}), according to the Randles–Sevcik equation [37]. The electroactive areas of the GCE and AuNPs-DHP/GCE were calculated to be 0.071 and 0.034 cm^2, respectively. Fig. 3(b) shows the CVs of the GCE and AuNPs-DHP/GCE at a scan rate of 100 mV s^{-1}. The GCE presented a higher electroactive area than the modified electrode, from which we conclude that the DHP can partly block the GCE, leading to a decrease in the electrochemical response. These results are in concordance

with recent studies published by Janegitz and co-workers [15] and Chikae and co-workers [7] that also proposed electrodes modified with AuNPs.

3.2. Tyr-AuNPs-DHP/GCE biosensor

The AuNPs were employed in order to develop a sensitive Tyr biosensor to determine the concentration catechol, and the Tyr enzyme was immobilized covalently onto the AuNPs via CYS and GA [38, 39].

The voltammetric behavior of the biosensor in the presence of catechol was studied. Fig. 4(a) presents the CVs of AuNPs-DHP/GCE and Tyr-AuNPs-DHP/GCE in 0.1 mol L^{-1} phosphate buffer solution (pH 6.0) in the presence of 1.0×10^{-4} mol L^{-1} catechol at a scan rate of 100 mV s^{-1}. We can observe that AuNPs-DHP/GCE presented a redox couple with similar intensity. In the same conditions, Tyr-AuNPs-DHP/GCE presented a decrease in the oxidation peak and an increase in the reduction peak almost three-fold. Besides, we can highlight that has occurred a displacement of the reduction peak to a negative potential. In fact, the Tyr catalyzes the oxidation of catechol to *o*-quinone in the presence of molecular oxygen. Therefore, *o*-quinone is reduced, thus regenerating the catechol at the electrode surface and increasing the analytical signal.

We also studied the effect of the scan rate on the electrochemical response of Tyr-AuNPs-DHP/GCE in the presence of 1.0×10^{-4} mol L^{-1} catechol in 0.1 mol L^{-1} phosphate buffer solution (pH 6.0). Fig. 4(b) shows that there was a slight displacement between the cathodic peaks as the scan rate increased, and a linear relationship between the cathodic peak current and the scan rate in the range 10 to 200 mV s^{-1} was observed, which indicates that the reaction occurred at the redox monolayer in the proposed electrode [30, 31, 40].

We recorded the influence of pH on the cathodic peak current of Tyr-AuNPs-DHP/GCE in the presence of 1.0×10^{-4} mol L^{-1} catechol and different 0.1 mol L^{-1} phosphate buffer solutions (pH in the range 5.0 to 7.0) at a scan rate of 100 mV s^{-1}. The cathodic peak current increased when in low values of pH up to 5.5, which presented the highest peak current. However, pH 6.0 was selected for further studies because it presented a high and reproducible analytical signal. The dependence between the cathodic peak and the pH was also evaluated. As can be observed in Fig. 4(c), the increase in pH leads to a negative shift in the potential of the cathodic peak current.

In order to determine catechol by amperometry, we studied the influence of the applied potential in the range 0.15 V to −0.35 V *vs.* Ag/AgCl in the presence of 5.0×10^{-5} mol L^{-1} catechol with stirring at 1100 rpm. The amperograms showed an increase in the cathodic current up to −0.10. V. In negative potentials, we did not find a significant increase in the analytical signal, which remained constant for other potentials. Thus, an applied potential of −0.10 V was chosen for further experiments.

3.3. Determination of catechol by amperometry

Under the optimal parameters we detected catechol by amperometry using the Tyr-AuNPs-DHP/GCE biosensor with stirring at 1100 rpm in the presence of 0.1 mol L^{-1} phosphate buffer solution (pH 6.0). The current increased linearly and proportionally with the catechol concentration in the range 2.5×10^{-6} to 9.5×10^{-5} mol L^{-1}, following the equation $I_c\,(\mu A) = -1.67 \times 10^{-8} + 1.15 \times 10^{5}$ [catechol] (mol L^{-1}) with a correlation coefficient of 0.999 (Fig. 5(a)). In addition, the proposed electrode presented a detection limit of 1.7×10^{-7} mol L^{-1} (based on three times the standard

deviation for the blank solution by the slope of the analytical curve).

The Tyr-AuNPs-DHP/GCE biosensor presented a lower detection limit (0.17 μmol L^{-1}) than several electrodes published in the literature, *e.g.*, Rajesh *et al.* [13] (1.2 μmol L^{-1}), Vicentini *et al.*[33] (0.58 μmol L^{-1}), Perez-Lopez *et al.* [41] (7.6 μmol L^{-1}), Dantoni *et al.* [42] (1.0 μmol L^{-1}), Solna *et al.* [43] (1.7 μmol L^{-1}), Tembe *et al.* [44] (6.0 μmol L^{-1}), Ozoner *et al.* [45] (0.67 μmol L^{-1}), Kheiri *et al.* [46] (0.8 μmol L^{-1}), and Apetrei *et al.* [47] (0.84 μmol L^{-1}), and very similar to others [14, 48-50]. The sensitivity using the proposed amperometric method (115 mA mol^{-1} L) was also higher than some biosensors applied for the same purpose, *e.g.*, Rajesh *et al.* [13] (3.5 mA mol^{-1} L), Yildiz *et al.* [14] (6.1 mA mol^{-1} L), Ozoner *et al.* [45] (8.0 mA mol^{-1} L), Perez-Lopez *et al.* [41] (4.8 mA mol^{-1} L), Apetrei *et al.* [47] (47 mA mol^{-1} L) and Sanz *et al.*[50] (107 mA mol^{-1} L). In addition, it is important to highlight that the proposed biosensor also presented high stability for long-term use as the response had only decreased to 93% after 30 days. The analytical parameters obtained in these procedures were compared with the novel amperometric method and was presented in Table 1.

In order to estimate the value of the rate of the enzyme-substrate intermediate dissociation without change of substrate to product (apparent Michaelis–Menten constant (K_M^{app})), which can be calculated by the Lineweaver–Burk plot (Fig. 5(b)), by the Lineweaver–Burk equation [15, 44], the equation $1/I_s$ = 0.0504 + 10.08 × 1/[catechol] (correlation coefficient of 0.998) was used, obtaining a K_M^{app} value of 0.20 mmol L^{-1}. This K_M^{app} value is in agreement with the literature [41, 50-56], which ranges

from 0.12 to 0.44; however, there are some electrodes that present a K_M^{app} higher than this range, *e.g.*, Smith *et al.* [57] (4.0 mmol L^{-1}) and Kiralp *et al.* [58] (100 and 200 mmol L^{-1}). The K_M^{app} value obtained with the Tyr-AuNPs-DHP/GCE biosensor leads us to conclude that the tyrosinase-immobilized AuNPs-DHP has a high catalytic activity and high affinity for catechol, which is related to an increase in the electron transfer rate.

We studied the repeatability of Tyr-AuNPs-DHP/GCE (n = 10) biosensor in the presence of 5.0×10^{-5} mol L^{-1} catechol and 0.1 mol L^{-1} phosphate buffer solution (pH 6.0). As can be seen in the Fig. 6, we obtained a relative standard deviation (RSD) of 0.5% for intra-day repeatability and 1.5% for inter-day repeatability. Moreover, we have also studied the repeatability for three different Tyr-AuNPs-DHP/GCE (repeatability of fabrication) that were prepared in the same way, and the voltammograms recorded in 5.0×10^{-5} mol L^{-1} catechol, and the RSD obtained was 3.8%.

The interference of species, such as potassium, magnesium, calcium, aluminum, iron, carbonate, chloride, phosphate, sulfate, bromide, iodide, and humic acids, was evaluated in the catechol determination using amperometry. All of these species, in presence of 5.0×10^{-5} mol L^{-1} catechol, presented interference of the proposed electrode of less than 5% across a 100-fold range of concentration (5.0×10^{-3} mol L^{-1}), indicating the electrode can be useful to determine catechol in water samples.

Tyr-AuNPs-DHP/GCE was used for the determination of catechol in water samples (natural water A, B, and C, and tap water D) using the standard addition method, and the recoveries were between 99% and 102 %. The results of the Tyr-AuNPs-DHP/GCE biosensors and those obtained by the reference method [34] are

shown in Table 2. Applying the paired *t* test for the obtained results, the calculated *t* was 2.176, which is smaller than the critical value (3.182, $\alpha = 0.05$), showing that there is no difference between the proposed and reference methods at a confidence level of 95%. Therefore, the Tyr-AuNPs-DHP/GCE method can be applied in catechol analysis of water samples.

In order to evaluate the long-term stability of the Tyr-AuNPs-DHP/GCE biosensor, we recorded the response of the electrode in the presence 5.0×10^{-5} mol L^{-1} catechol for one month (or 240 measurements). After this period, the response had decreased by 7.0%. This great stability can be related to two main factors: the effective enzymatic immobilization, and the biocompatibility between the Tyr enzyme and AuNPs in the biosensor.

4. Conclusions

The modified electrode with AuNPs presents advantages, including biocompatibility with the Tyr enzyme and an increase in the analytical signal for catechol. Amperometry was successfully applied for catechol determination using the proposed biosensor, which can be applied in samples, such as natural water samples and tap water. In addition, the electrode is easy to prepare and the proposed method could be extended to immobilize other enzymes for other biosensing applications.

Acknowledgments

The authors are grateful for the financial support from the Brazilian funding agencies FAPESP, CNPq, and CAPES. F.C. Vicentini and L.C.S Figueiredo-Filho are

particularly grateful to the São Paulo Research Foundation (FAPESP) for the award of postdoctoral scholarships (Proc. No. 2013/16770-0 and 2014/04284-6).

References

[1] Chomoucka J, Drbohlavova J, Masarik M, Ryvolova M, Huska D, Prasek J, Horna A, Trnkova L, Provaznik I, Adam V, Hubalek J, Kizek R. Nanotechnologies for society. New designs and applications of nanosensors and nanobiosensors in medicine and environmental analysis. Int J Nanotechnol. 2012;9:746-83.

[2] Jones SEW, Compton RG. Fabrication and applications of nanoparticle-modified electrodes in stripping analysis. Curr Anal Chem. 2008;4:177-82.

[3] Marin S, Merkoci A. Nanomaterials based electrochemical sensing applications for safety and security. Electroanalysis. 2012;24:459-69.

[4] Compton RG, Wildgoose GG, Rees NV, Streeter I, Baron R. Design, fabrication, characterisation and application of nanoelectrode arrays. Chem Phys Lett. 2008;459:1-17.

[5] Welch CW, Compton RG. The use of nanoparticles in electroanalysis: a review. Anal Bioanal Chem. 2006;384:601-19.

[6] Sartori ER, Vicentini FC, Fatibello-Filho O. Indirect determination of sulfite using a polyphenol oxidase biosensor based on a glassy carbon electrode modified with multi-walled carbon nanotubes and gold nanoparticles within a poly(allylamine hydrochloride) film. Talanta. 2011;87:235-42.

[7] Chikae M, Idegami K, Kerman K, Nagatani N, Ishikawa M, Takamura Y, Tamiya E. Direct fabrication of catalytic metal nanoparticles onto the surface of a screen-printed carbon electrode. Electrochem Commun. 2006;8:1375-80.

[8] Jiang KY, Eitan A, Schadler LS, Ajayan PM, Siegel RW, Grobert N, Mayne M, Reyes-Reyes M, Terrones H, Terrones M. Selective attachment of gold nanoparticles to nitrogen-doped carbon nanotubes. Nano Lett. 2003;3:275-7.

[9] Pingarron JM, Yanez-Sedeno P, Gonzalez-Cortes A. Gold nanoparticle-based electrochemical biosensors. Electrochim Acta. 2008;53:5848-66.

[10] Putzbach W, Ronkainen NJ. Immobilization techniques in the fabrication of nanomaterial-based electrochemical biosensors: a review. Sensors. 2013;13:4811-40.

[11] Lin YC, Yu BY, Lin WC, Lee SH, Kuo CH, Shyue JJ. Tailoring the surface potential of gold nanoparticles with self-assembled monolayers with mixed functional groups. J Colloid Interface Sci. 2009;340:126-30.

[12] Liu Z, Liu J, Shen G, Yu R. A reagentless tyrosinase biosensor based on 1,6-hexanedithiol and nano-Au self-assembled monolayers. Electroanalysis. 2006;18:1572-7.

[13] Rajesh, Takashima W, Kaneto K. Amperometric phenol biosensor based on covalent immobilization of tyrosinase onto an electrochemically prepared novel copolymer poly (N-3-aminopropyl pyrrole-co-pyrrole) film. Sens Actuators B. 2004;102:271-7.

[14] Yildiz HB, Castillo J, Guschin DA, Toppare L, Schuhmann W. Phenol biosensor based on electrochemically controlled integration of tyrosinase in a redox polymer. Microchim Acta. 2007;159:27-34.

[15] Janegitz BC, Medeiros RA, Rocha-Filho RC, Fatibello-Filho O. Direct electrochemistry of tyrosinase and biosensing for phenol based on gold nanoparticles electrodeposited on a boron-doped diamond electrode. Diam Relat Mat. 2012;25:128-33.

[16] Kochana J, Gala A, Parczewski A, Adamski J. Titania sol-gel-derived tyrosinase-based amperometric biosensor for determination of phenolic compounds in water samples. Examination of interference effects. Anal Bioanal Chem. 2008;391:1275-81.

[17] Karim F, Fakhruddin ANM. Recent advances in the development of biosensor for phenol: a review. Rev Environ Sci Bio-Technol. 2012;11:261-74.

[18] Fiorentino D, Gallone A, Fiocco D, Palazzo G, Mallardi A. Mushroom tyrosinase in polyelectrolyte multilayers as an optical biosensor for o-diphenols. Biosens Bioelectron. 2010;25:2033-7.

[19] Hanefeld U, Gardossi L, Magner E. Understanding enzyme immobilisation. Chem Soc Rev. 2009;38:453-68.

[20] Alfaya AAS, Kubota LT. The utilization of materials obtained by the sol-gel process in biosensors construction. Quim Nova. 2002;25:835-41.

[21] Jia JB, Wang BQ, Wu AG, Cheng GJ, Li Z, Dong SJ. A method to construct a third-generation horseradish peroxidase biosensor: Self-assembling gold nanoparticles to three-dimensional sol-gel network. Anal. Chem. 2002;74:2217-23.

[22] Carpani I, Scavetta E, Tonelli D. Amperometric glucose biosensors based on glassy carbon and SWCNT-modified glassy carbon electrodes. Electroanalysis. 2008;20:84-90.

[23] Topkaya SN. Gelatin methacrylate (GelMA) mediated electrochemical DNA biosensor for DNA hybridization. Biosens Bioelectron. 2015;64:456-61.

[24] Kesik M, Kanik FE, Turan J, Kolb M, Timur S, Bahadir M, Toppare L. An acetylcholinesterase biosensor based on a conducting polymer using multiwalled carbon nanotubes for amperometric detection of organophosphorous pesticides. Sens Actuators B. 2014;205:39-49.

[25] Cipolatti EP, Silva MJA, Klein M, Feddern V, Feltes MMC, Oliveira JV, Ninow JL, Oliveira D. Current status and trends in enzymatic nanoimmobilization. J Mol Catal B-Enzym. 2014;99:56-67.

[26] Wu YH. Nano-TiO_2/dihexadecylphosphate based electrochemical sensor for sensitive determination of pentachlorophenol. Sens Actuators B. 2009;137:180-4.

[27] Vicentini FC, Elisa Ravanini A, Silva TA, Janegitz BC, Zucolotto V, Fatibello-Filho O. A novel architecture based upon multi-walled carbon nanotubes and ionic liquid to improve the electroanalytical detection of ciprofibrate. Analyst. 2014;139:3961-7.

[28] Yao SJ, Xu JH, Wang Y, Chen XX, Xu YX, Hu SS. A highly sensitive hydrogen peroxide amperometric sensor based on MnO_2 nanoparticles and dihexadecyl hydrogen phosphate composite film. Anal Chim Acta. 2006;557:78-84.

[29] Figueiredo-Filho LCS, Silva TA, Vicentini FC, Fatibello-Filho O. Simultaneous voltammetric determination of dopamine and epinephrine in human body fluid samples using a glassy carbon electrode modified with nickel oxide nanoparticles and carbon nanotubes within a dihexadecylphosphate film. Analyst. 2014;139:2842-9.

[30] Janegitz BC, Pauliukaite R, Ghica ME, Brett CMA, Fatibello-Filho O. Direct electron transfer of glucose oxidase at glassy carbon electrode modified with functionalized carbon nanotubes within a dihexadecylphosphate film. Sens Actuators B. 2011;158:411-7.

[31] Wu YH, Hu SS. Direct electrochemistry of glucose oxidase in a colloid Au-dihexadecylphosphate composite film and its application to develop a glucose biosensor. Bioelectrochemistry. 2007;70:335-41.

[32] Kashanian S, Tarighat FA, Rafipour R, Abbasi-Tarighat M. Biomimetic synthesis and characterization of cobalt nanoparticles using apoferritin, and investigation of direct electron transfer of Co(NPs)-ferritin at modified glassy carbon electrode to design a novel nanobiosensor. Mol Biol Rep. 2012;39:8793-802.

[33] Vicentini FC, Janegitz BC, Brett CMA, Fatibello-Filho O. Tyrosinase biosensor based on a glassy carbon electrode modified with multi-walled carbon nanotubes and 1-

butyl-3-methylimidazolium chloride within a dihexadecylphosphate film. Sens Actuators B. 2013;188:1101-8.

[34] Greenberg AE, Clesceri LS, Eaton AD. Standard Methods for the Examination of Water and Wastewater. 19th ed. USA: American Public Health Association; 1995.

[35] Turkevich J, Stevenson PC, Hillier J. A study of the nucleation and growth processes in the synthesis of colloidal gold. Discuss Faraday Soc. 1951:55-75.

[36] Wang Y, Laborda E, Crossley A, Compton RG. Surface oxidation of gold nanoparticles supported on a glassy carbon electrode in sulphuric acid medium: contrasts with the behaviour of 'macro' gold. Phys Chem Chem Phys. 2013;15:3133-6.

[37] Brett CMA, Brett AMO. Electrochemistry: Principles, Methods and Applications. Oxford: Oxford University Press; 1993.

[38] Pauliukaite R, Ghica ME, Fatibello-Filho O, Brett CMA. Comparative study of different cross-linking agents for the immobilization of functionalized carbon nanotubes within a chitosan film supported on a graphite-epoxy composite electrode. Analytical Chemistry. 2009;81:5364-72.

[39] Fatibello-Filho O, Capelato MD. Biossensores. Quim Nova. 1992;15:28-39.

[40] Bard AJ, Faulkner LR. Electrochemical Methods: Fundamentals and Applications. 2 ed. New York: John Wiley & Sons Inc.; 2001.

[41] Perez-Lopez B, Merkoci A. Magnetic nanoparticles modified with carbon nanotubes for electrocatalytic magnetoswitchable biosensing applications. Adv Funct Mater. 2011;21:255-60.

[42] Dantoni P, Serrano SHP, Oliveira-Brett AM, Gutz IGR. Flow-injection determination of catechol with a new tyrosinase/DNA biosensor. Anal Chim Acta. 1998;366:137-45.

[43] Solna R, Sapelnikova S, Skladal P, Winther-Nielsen M, Carlsson C, Emneus J, Ruzgas T. Multienzyme electrochemical array sensor for determination of phenols and pesticides. Talanta. 2005;65:349-57.

[44] Tembe S, Inamdar S, Haram S, Karve M, D'Souza SF. Electrochemical biosensor for catechol using agarose-guar gum entrapped tyrosinase. J Biotechnol. 2007;128:80-5.

[45] Ozoner SK, Yalvac M, Erhan E. Flow injection determination of catechol based on polypyrrole-carbon nanotube-tyrosinase biocomposite detector. Curr Appl Phys. 2010;10:323-8.

[46] Kheiri F, Sabzi RE, Jannatdoust E, Sedghi H. Acetone extracted propolis as a novel membrane and its application in phenol biosensors: the case of catechol. J Solid State Electrochem. 2011;15:2593-9.

[47] Apetrei C, Rodriguez-Mendez ML, De Saja JA. Amperometric tyrosinase based biosensor using an electropolymerized phosphate-doped polypyrrole film as an immobilization support. Application for detection of phenolic compounds. Electrochim Acta. 2011;56:8919-25.

[48] Tan YY, Kan JQ, Li SQ. Amperometric biosensor for catechol using electrochemical template process. Sens Actuators B. 2011;152:285-91.

[49] Han RX, Cui L, Ai SY, Yin HS, Liu XG, Qiu YY. Amperometric biosensor based on tyrosinase immobilized in hydrotalcite-like compounds film for the determination of polyphenols. J Solid State Electrochem. 2012;16:449-56.

[50] Carralero Sanz V, Mena ML, González-Cortés A, Yáñez-Sedeño P, Pingarrón JM. Development of a tyrosinase biosensor based on gold nanoparticles-modified glassy carbon electrodes: Application to the measurement of a bioelectrochemical polyphenols index in wines. Anal Chim Acta. 2005;528:1-8.

[51] Ji XP, Li XR, Wang N, Ni RX, Liu XH, Xiong HA. Attachment of tyrosinase on mixed self-assembled monolayers for the construction of electrochemical biosensor. Chin Chem Lett. 2010;21:1239-42.

[52] Burestedt E, Narvaez A, Ruzgas T, Gorton L, Emneus J, Dominguez E, Marko-Varga G. Rate-limiting steps of tyrosinase-modified electrodes for the detection of catechol. Anal. Chem. 1996;68:1605-11.

[53] Serra B, Jimenez S, Mena ML, Reviejo AJ, Pingarron JM. Composite electrochemical biosensors: a comparison of three different electrode matrices for the construction of amperometric tyrosinase biosensors. Biosens Bioelectron. 2002;17:217-26.

[54] Brown RS, Male KB, Luong JHT. A substrate recycling assay for phenolic-compounds using tyrosinase and NADH. Anal Biochem. 1994;222:131-9.

[55] Campuzano S, Serra B, Pedrero M, de Villena FJM, Pingarron JM. Amperometric flow-injection determination of phenolic compounds at self-assembled monolayer-based tyrosinase biosensors. Anal Chim Acta. 2003;494:187-97.

[56] Espin JC, Morales M, Garcia-Ruiz PA, Tudela J, Garcia-Canovas F. Improvement of a continuous spectrophotometric method for determining the monophenolase and

diphenolase activities of mushroom polyphenol oxidase. J Agric Food Chem. 1997;45:1084-90.

[57] Smith JL, Krueger RC. Separation and purification of phenolases of common mushroom. J Biol Chem. 1962;237:1121-8.

[58] Kiralp S, Toppare L, Yagci Y. Immobilization of polyphenol oxidase in conducting copolymers and determination of phenolic compounds in wines with enzyme electrodes. Int J Biol Macromol. 2003;33:37-41.

Figure Captions

Fig. 1. Scheme of the preparation of the Tyr-AuNPs-DHP/GCE biosensor.

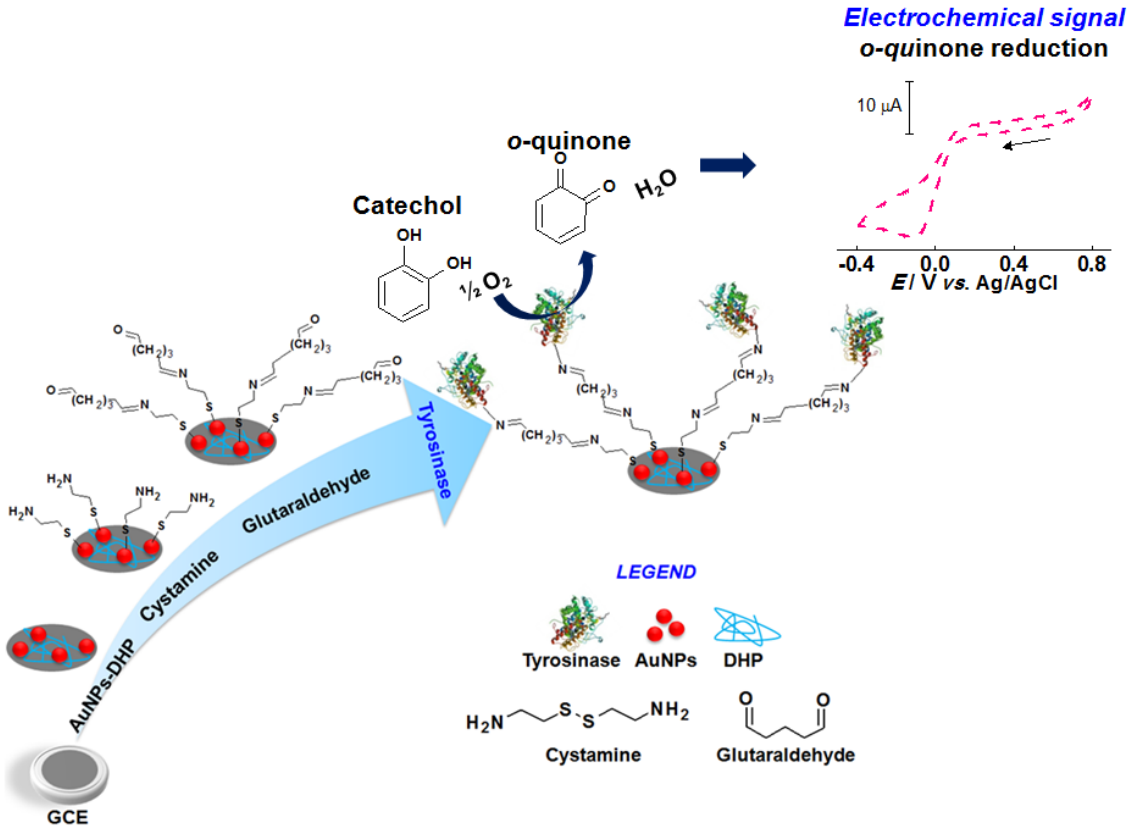

Fig. 2. SEM images of GCE (a) and AuNPs-DHP/GCE (b). TEM image of AuNPs (c) and the corresponding histogram of the AuNPs diameters (d). The solid line corresponds to the Gaussian fit.

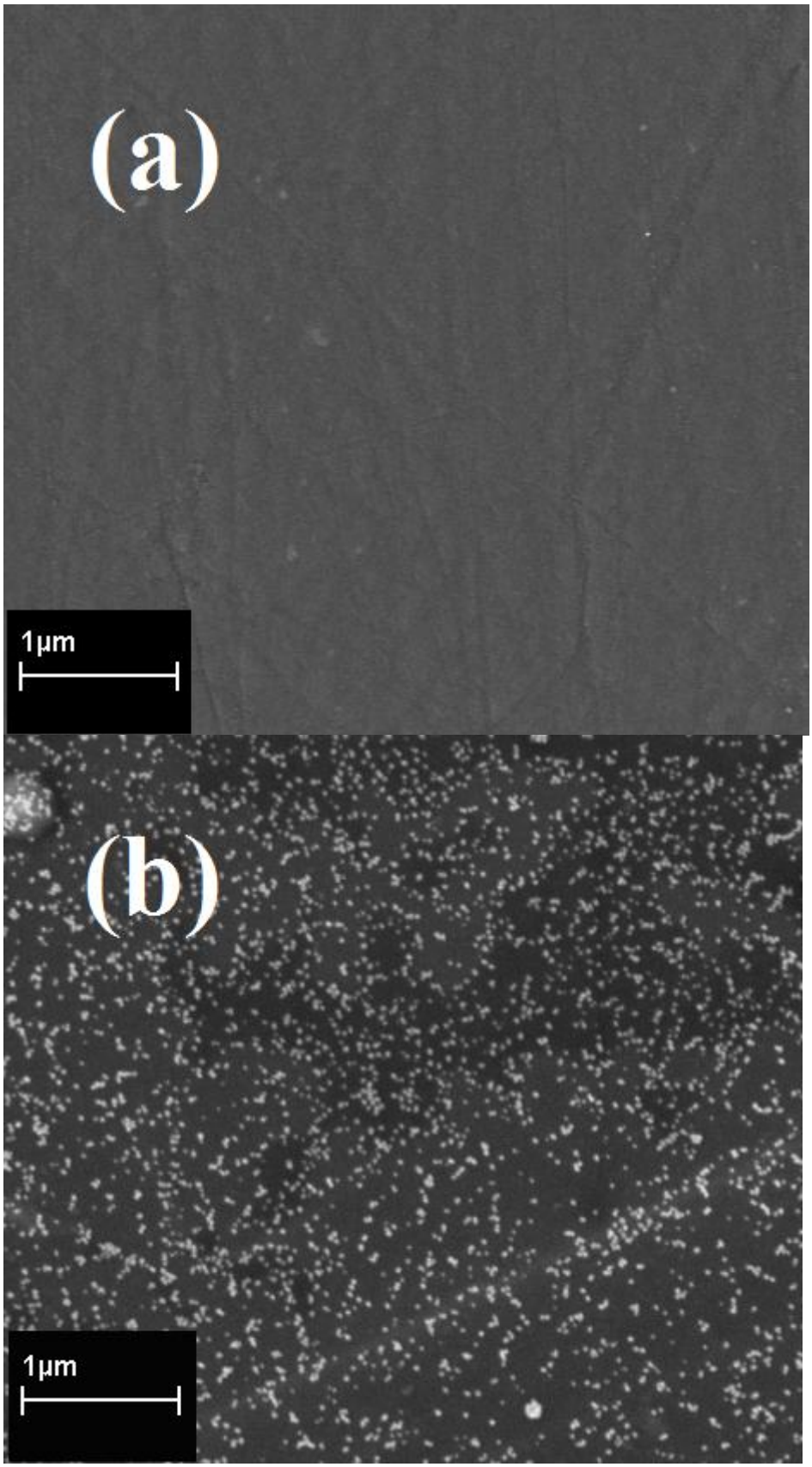

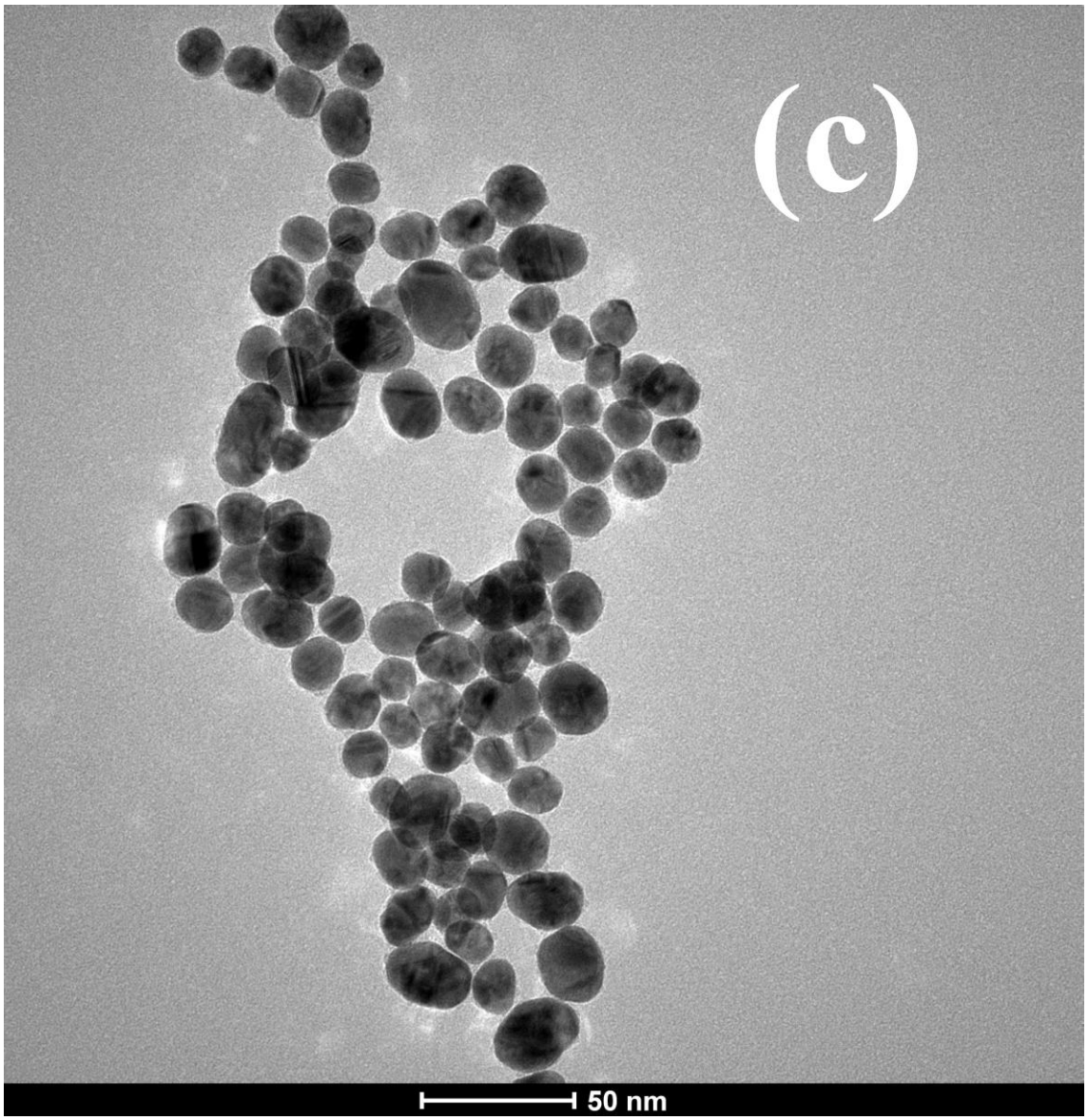

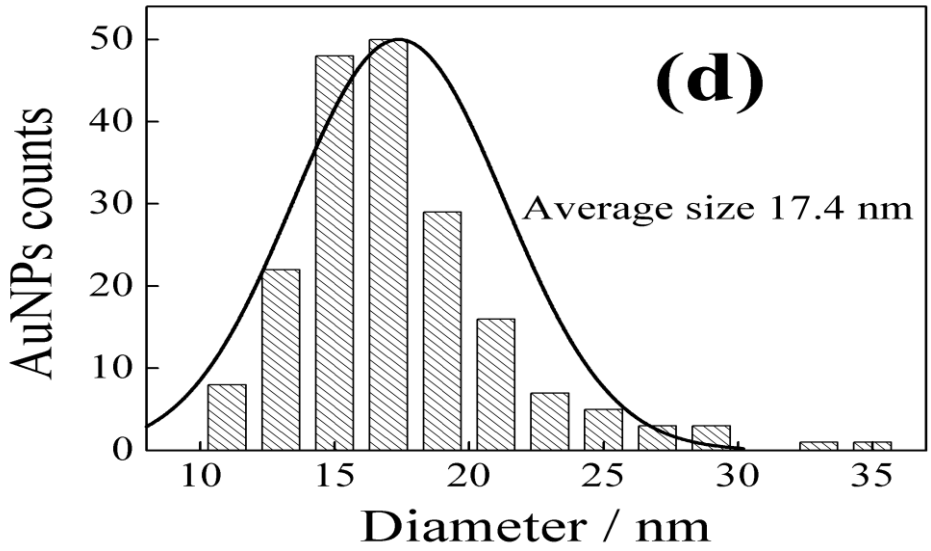

Fig. 3. (a) CV of AuNPs-DHP/GCE in 0.5 mol L^{-1} H_2SO_4 solution, at a scan rate of 50 mV s^{-1}, (b) CVs of GCE (–) and AuNPs-DHP/GCE (–) in the presence of 1.0×10^{-3} mol L^{-1} $[Fe(CN)_6]^{4-}$ in 0.1 mol L^{-1} KCl, at a scan rate of 100 mV s^{-1}.

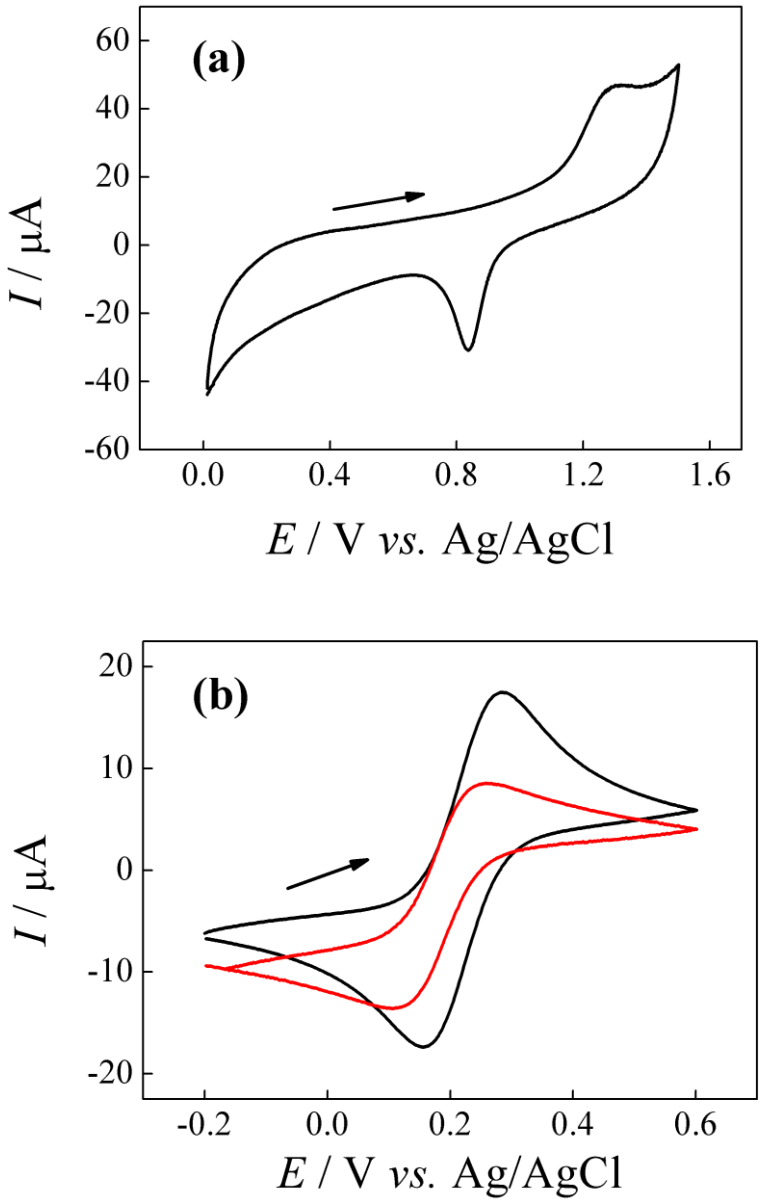

Fig. 4. (a) CVs of AuNPs-DHP/GCE (**–**) and Tyr-AuNPs-DHP/GCE (**–**) in 0.1 mol L^{-1} phosphate buffer solution (pH 6.0) in presence of 1.0×10^{-4} mol L^{-1} catechol at a scan rate of 100 mV s^{-1}. (b) CVs of Tyr-AuNPs-DHP/GCE at scan rates of 10, 20, 30, 40, 50, 75, 100, 150, and 200 mV s^{-1} in the presence of 1.0×10^{-4} mol L^{-1} catechol in 0.1 mol L^{-1} phosphate buffer solution (pH 6.0). Inset *I vs. v*. (c) CVs of Tyr-AuNPs-DHP/GCE in the presence of 1.0×10^{-4} mol L^{-1} catechol in 0.1 mol L^{-1} phosphate buffer solution in pH ranging from 5.0 to 7.0, at a scan rate of 100 mV s^{-1}. Inset: $-I_{pc}$ *vs.* pH.

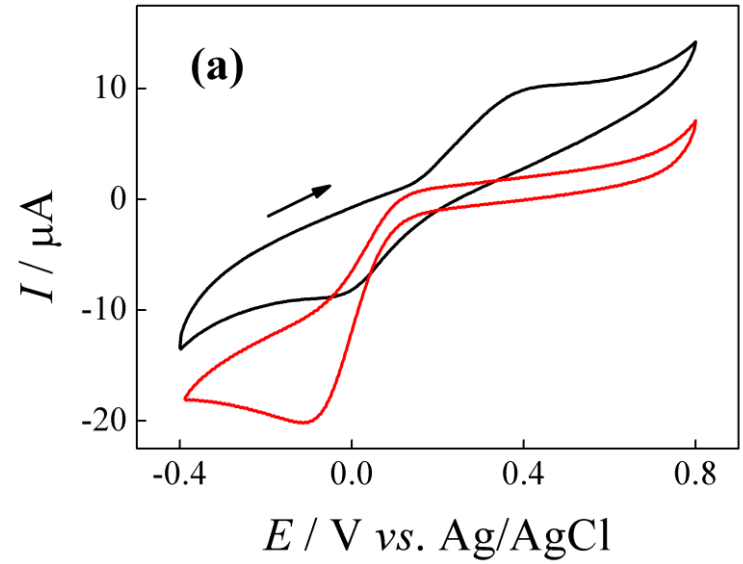

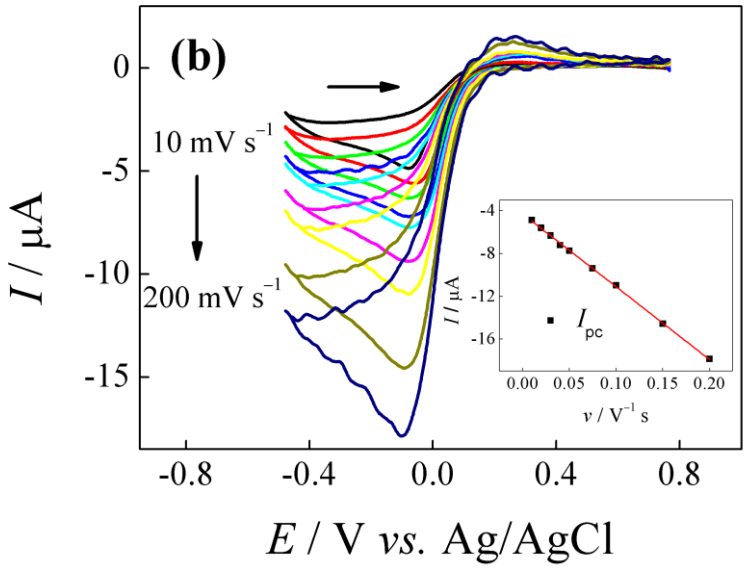

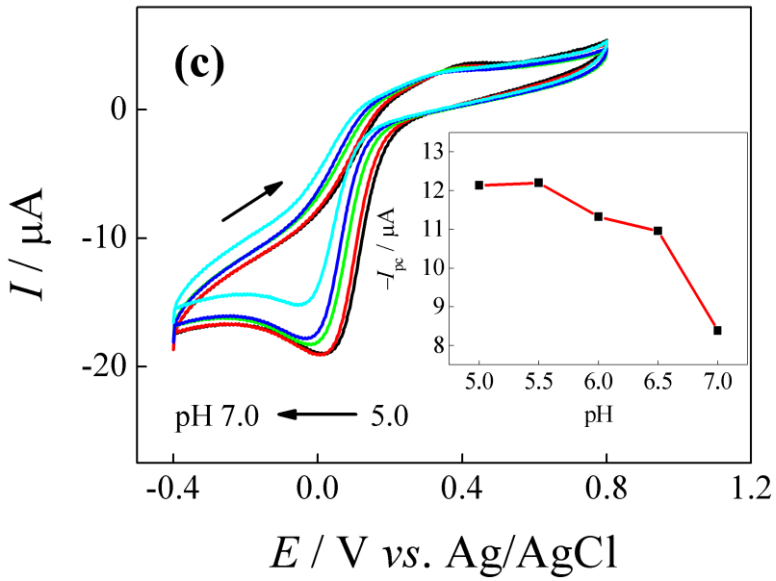

Fig. 5. (a) Amperogram obtained using the Tyr-AuNPs-DHP/GCE biosensor in 0.1 mol L^{-1} phosphate buffer solution (pH 6.0), E_c = −0.10 V, in the presence of 2.5 × 10^{-6} (1), 3.7 × 10^{-6} (2), 5.0 × 10^{-6} (3), 6.2 × 10^{-6} (4), 7.4 × 10^{-6} (5), 1.5 × 10^{-5} (6), 2.2 × 10^{-5} (7), 2.9 × 10^{-5} (8), 3.6 × 10^{-5} (9), 4.3 × 10^{-5} (10), 5.0 × 10^{-5} (11), 5.7 × 10^{-5} (12), 6.3 × 10^{-5} (13), 7.0 × 10^{-5} (14), 7.6 × 10^{-5} (15), 8.3 × 10^{-5} (16), 8.8 × 10^{-5} (17), and 9.5 × 10^{-5} (18) mol L^{-1} catechol. Analytical curve is inset. (b) Corresponding Lineweaver–Burk plot.

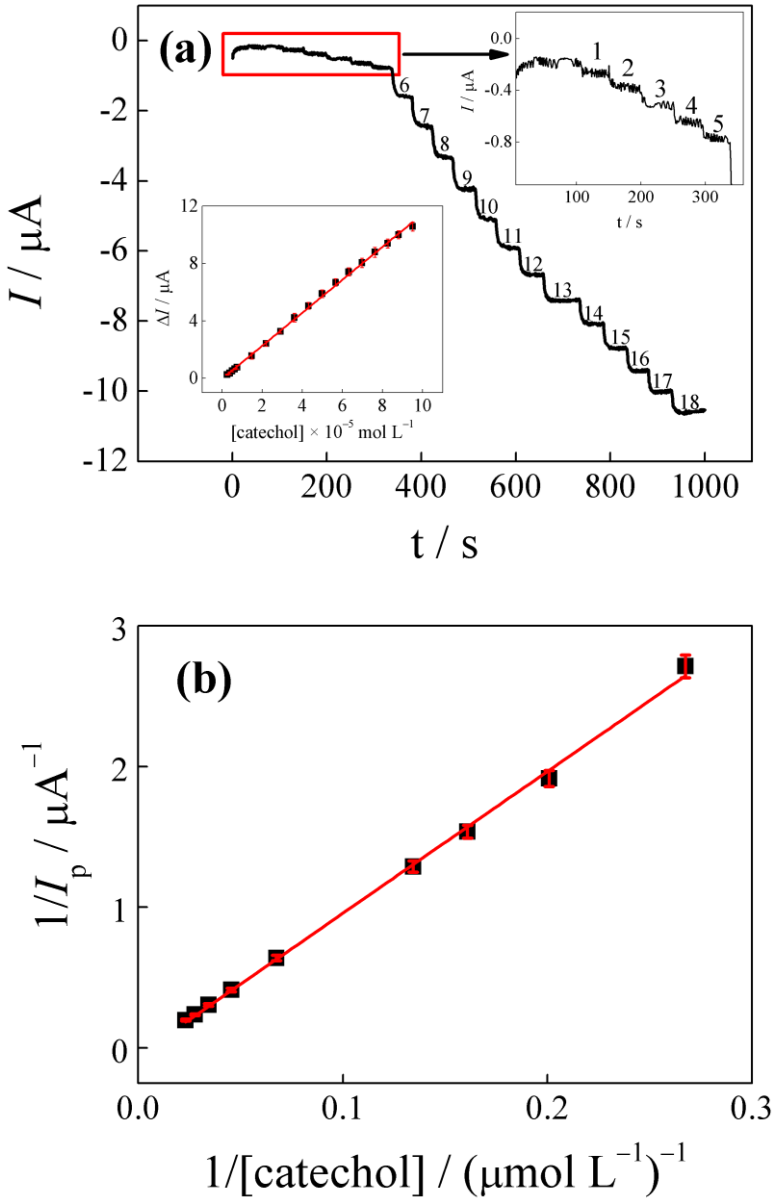

Fig. 6. Repeatability studies using the proposed Tyr-AuNPs-DHP/GCE biosensor in the presence of 5.0×10^{-5} mol L^{-1} catechol and 0.1 mol L^{-1} phosphate buffer solution (pH 6.0).

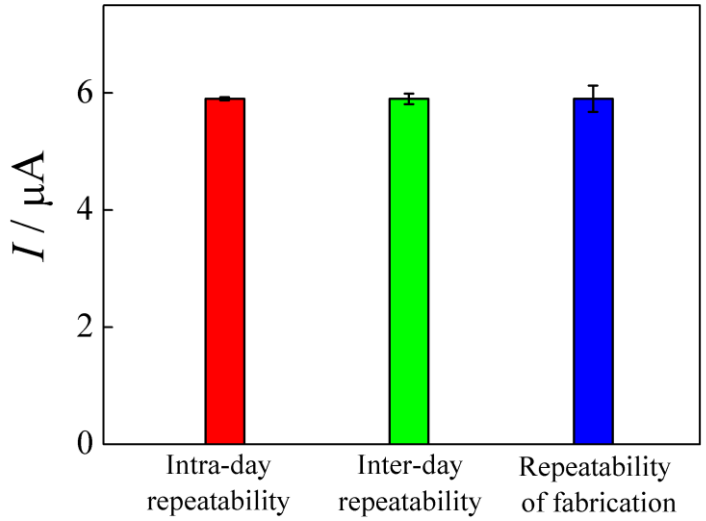

Table 1 Comparison between the analytical parameters obtained for the proposed amperometric procedure and other electroanalytical procedures reported in the literature for catechol determination

Electrode	**Linear range ($\mu mol\ L^{-1}$)**	**Detection Limit ($\mu mol\ L^{-1}$)**	Sensitivity **($mA\ mol^{-1}\ L$)**	Stability	Reference
Tyr-PAPCP/ITO	1.6 – 140	1.2	3.5	80% remained after 120 days	[13]
Tyr-Oscomplex-functionalized/Pt	–	0.01	6.1	–	[14]
Tyr-IL-MWCNT-DHP/GCE	4.9 – 1100	0.58	32.8	95% remained after 30 days	[33]
Tyr-MWCNT-MNP/SPE	10 – 80	7.6	4.8	Shelf life: 1 month	[41]
Tyr-DNA/CP	1.0 – 50	1.0	–	Shelf life: 2 months	[42]
Tyr/SPPtE	–	1.7	–	50-60% after 150 measurements	[43]
Tyr-Agarose-guar gum/GCE	60 – 800	6.0	–	Shelf life: 2 months	[44]
Tyr-MWCNT-PPy/GCE	3.0 – 50	0.67	8.0	85% remained after 70 days	[45]
Tyr/MWCNT/AuNPs/AEP/Au	1.0 – 500	0.8	150	80% remained after 42 days	[46]
Tyr-PO_4–PPy/Pt	10 – 120	0.84	47	80% remained after 30 days	[47]
Tyr-PANI/Pt	5.0 – 140	0.05	–	90% remained after 120 days	[48]
Tyr-HTLc/GCE	3.0 – 300	0.1	–	72% remained after 30 days	[49]
Tyr-nAu/GCE	0.5 – 50	0.15	107	Shelf life: 18 days	[50]
Tyr-AuNPs-DHP/GCE	2.5 – 95	0.17	115	93% remained after 30 days	This work

PAPCP: Poly (*N*-3-aminopropyl pyrrole-co-pyrrole); ITO: indium-tin-oxide; Os: Osmium; IL: Ionic liquid; MWCNT: Multi-walled carbon nanotube; MNP: Magnetic nanoparticles; CP: Carbon paste; SPPtE: Screen-printed Pt electrode; PPy: Polypyrrole; AuNPs: Gold nanoparticles; AEP: Acetone-extracted propolis; Au: Gold electrode; Pt: Platinum electrode; PANI: polyaniline; HTLc: Mg–Al–CO_3 hydrotalcite-like; nAu: electrodeposited gold nanoparticles.

Table 2: Catechol determination using the Tyr-AuNPs-DHP/GCE biosensor and the spectrophotometric method [34]

Sample	Catechol (10^{-6} mol L^{-1})		
	Reference method*	**Proposed method**	**Relative error****
A	49.1 ± 0.3	50.8 ± 0.3	+3.5
B	47.4 ± 0.4	49.5 ± 0.2	+4.4
C	48.7 ± 0.2	51.1 ± 0.4	+4.9
D	51.0 ± 0.2	50.5 ± 0.1	−1.0

* Spectrophotometric method− average of 3 measurements

** [(Proposed method – reference method) × 100]/ reference method.